Analyst

Accepted Manuscript

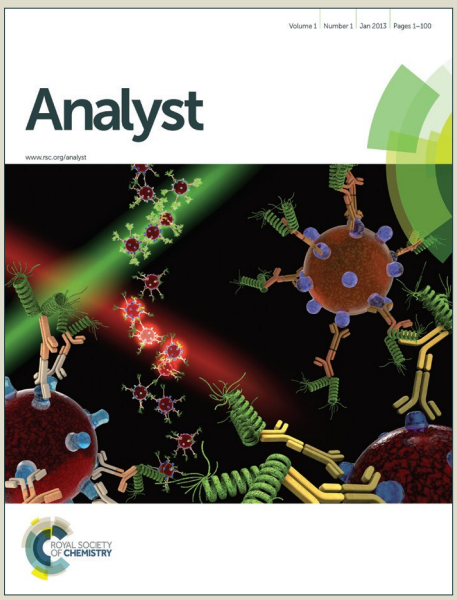

ROYAL SOCIETY OF CHEMISTRY

www.rsc.org/analyst

Multiple gas-phase conformations of proline-containing peptides: Is it always *cis*/*trans* isomerization?

Christopher B. Lietz,[a] Zhengwei Chen,[a] Chang Yun Son,[a] Xueqin Pang,[b] Qiang Cui,[a] and Lingjun Li[a,b,*]

[a]Department of Chemistry, University of Wisconsin-Madison, 1101 University Avenue, Madison, WI, 53706

[b]School of Pharmacy, University of Wisconsin-Madison, 777 Highland Avenue, Madison, WI, 53705

***Correspondence:** Professor Lingjun Li, School of Pharmacy and Department of Chemistry, University of Wisconsin–Madison, 777 Highland Avenue, Madison, Wisconsin 53705-2222

E-mail: lingjun.li@wisc.edu

Fax: +1-608-262-5345

Abstract

Ion mobility-mass spectrometry (IM-MS) is often employed to look at the secondary, tertiary, and quaternary structure of naked peptides and proteins in the gas-phase. Recently, it has offered a unique glimpse into proline-containing peptides and their cis/trans Xxx-Pro isomers. An experimental "signature" has been identified wherein a proline-containing peptide has its Pro residues substituted with another amino acid and the presence or absence of conformations in the IM-MS spectra are observed. Despite high probability that one could attribute these conformations to cis/trans isomers, it is also possible that cis/trans isomers are not the cause of the additional conformations in proline-containing peptides. However, the experimental evidence of such a system has not been demonstrated or reported. Herein, we present the IM-MS analysis of Neuropeptide Y's wild-type (WT) signal sequence and Leu7Pro (L7P) mutant. Although comparison of arrival times and collision cross sections of $[M+4H]^{4+}$ ions yield the cis/trans "signature", molecular dynamics indicates that a cis-Pro7 is not very stable and that trans-Pro7 conformations of the same cross section arise with equal frequency. We believe this work further underscores the importance of theoretical calculations in IM-MS structural assignments.

Ion mobility (**IM**)-mass spectrometry (**MS**) is a gas-phase electrophoretic separation method. Ions are pulled through a buffer gas by a weak electric field and separated by charge and collision cross section (**CCS**).[1] As its implementation expands, IM-MS continues to establish itself as an important tool for the structural characterization of biomolecules.[2-7] One area to which it has provided particular advantage is the analysis of small, flexible, highly disordered peptides. When careful measures are taken to ensure gentle ionization and ion transport, IM-MS can help identify the distributions of preferred peptide conformations and intermediates that may not be resolved in more traditional techniques like NMR.[8]

Proline-containing peptides,[9-14] small proline-containing proteins,[15-16] and derivatized proline amino acids[17] have been a frequent target of IM-MS studies. Through the creation and analysis of a large database, Counterman and Clemmer were the first to reveal that tryptic peptides containing proline were more likely to display multiple IM peaks than those without proline.[18] The investigation ultimately suggested that these multiple peaks arose from populations of cis-proline and trans-proline isomers. Therefore, they proposed peptide ions with both cis- and trans-proline may be relatively common in the gas-phase.

In a later study, Pierson et al. developed a method to more accurately catalogue which IM peaks originated from cis/trans isomers.[19] The IM-MS spectrum of a proline-containing peptide is compared to the IM-MS spectrum of the same peptide but with its proline residues substituted with a different amino acid (for example, APAAA and AxAAA, where $x \neq P$). Since proline is unique in its ability to have appreciable populations of cis peptide bonds,[20] IM peaks shared with the substituted peptide are thought to emerge from trans-proline conformations, and peaks unique to the proline-containing peptide are thought to come from cis-proline conformations. This approach helped to solidify the experimental IM-MS "signature" of cis/trans prolines and

led to novel insights into the energetics of isomerization[21] and the effect of proline sequence position.[22-23]

Proline isomerization plays a crucial role in the rate of protein folding.[20] Although IM-MS could play a complementary role for proline analysis in peptide and protein systems, investigators often show prudence by mentioning the possibility that proline-induced multiple conformation may arise from events other than cis/trans isomerization. Therefore, cis/trans proline experiments often incorporate molecular dynamics (**MD**) simulations[24-26] to garner further support for specific designations of cis or trans conformations. Briefly, MD simulations are run in parallel with IM-MS data collection. The theoretical CCS of structures obtained from MD are then matched to the calculated CCS of ions observed in experiments. To our knowledge, no study has presented evidence for phenomena other than cis/trans-isomerization in the appearance of multiple peptide conformations after proline-substitution.

Here, we present the investigation of a proline-containing peptide system with the experimental hallmarks of cis/trans-proline conformers. We hypothesized isomerization as the explanation, but theoretical simulations yielded evidence for an all trans-proline explanation. Given the rise in use and maturation of commercial IM-MS instruments, we believe such a communication is important to provide a concrete example of what previous reports have cautioned.

We chose the 28-residue wild-type signal sequence of Neuropeptide Y (**NPY**) (MLGNKR**L**GLSGLTLALSLLVCLGALAEA), hereafter referred to as WT, and its naturally-occurring Leu7Pro mutant (MLGNKR**P**GLSGLTLALSLLVCLGALAEA), hereafter referred to as L7P, for use in this study. The peptides only differ in the identity of the seventh residue: Leu7

for WT and a Pro7 for L7P. Because of the proline substitution, this system has the potential for displaying the IM-MS signatures of cis/trans isomerization.

It is interesting to note that the L7P mutation has strong biological consequences. NPY is initially translated as an inactive pro-hormone, called pro-NPY, and is guided by its N-terminal signal sequence to the endoplasmic reticulum for processing into bioactive NPY.[27] Upon entry into the endoplasmic reticulum, the signal sequence is cleaved from pro-NPY by signal peptidases. As a result of unknown molecular mechanisms, individuals with the L7P mutation have higher levels of bioactive NPY in their blood serum and are more likely to suffer from medical conditions such as diabetes than individuals with the WT sequence.[28-31]

Figure 1 shows the sequences of the WT and L7P peptides and their nano electrospray ionization (**ESI**) mass spectra. All IM-MS was performed by direct infusion on a Waters SYNAPT G2 HDMS nano ESI source from analyte solutions in 50:50 water:methanol. Further details can be found in **Supplemental Information 1**. As seen in **Figure 1B**, the most abundant ion species in both spectra are the triply protonated monomers. An inset of the yellow region near *m*/*z* 700 is shown in **Figure 1C** and **Figure 1D.** They contain 4+ L7P and WT monomers, respectively. Both peptides displayed peaks of slightly higher abundance corresponding to $[M+3H+K]^{4+}$ compared to the $[M+4H]^{4+}$ ions (labeled as $L7P^{4+}$ or WT^{4+}). **Figure 1E** and **Figure 1F** show the green-highlighted region near *m*/*z* 1400. These spectra contain the 2+ monomers and low abundance signals from 4+ dimers.

Since protonated monomers were observed for all charge states, we focused further analysis on ions of this type. Subsequently, IM arrival time distributions (**ATDs**) were acquired and calibrated CCS were calculated to search for evidence of cis/trans isomers. We hypothesized that peaks with nearly identical CCS common to both WT and L7P may represent

similar conformations with the seventh residue in a trans peptide bond, and additional peaks unique to L7P may indicate a cis Arg6-Pro7 bond. It is important to note that we cannot directly calculate CCS from ATDs acquired on our unmodified SYNAPT G2.[32] We utilized ions with known CCS and a common calibration strategy[33-35] to calculate calibrated CCS for WT and L7P. Our group has previously used this method and obtained peptide CCS with under 3% error.[13]

The ATDs and calibrated CCS of the 2+ and 3+ ions are shown in **Figure S1**. At these charge states, we did not see any convincing evidence of cis/trans isomers. The full-width-half-maximum Arrival Time resolution values for the primary 2+ and 3+ peaks are 19.2 and 17.4, respectively. The resolution of the 3+ peak, in particular, is lower than what would be expected for a single IM feature on this instrument.[36] Combined with the presence of a low-abundance "shoulder peak" later in the ATD, we cannot discount the possibility that high resolution instrumentation may reveal a cis/trans-like signature.

Figure 2 shows the ATDs and calibrated CCS of the 4+ WT and L7P ions. These spectra have a very different appearance than their 2+ and 3+ counterparts. Both peptides display a single narrow peak with identical mean CCS of 527 $Å^2$, as well as more extended conformations at 626 $Å^2$ (WT) and 627 $Å^2$ (L7P). Additionally, the $L7P^{4+}$ spectrum contains a third peak at 610 $Å^2$. This was precisely the type of IM-MS profile that would suggest the presence of cis-proline and trans-proline isomers. Therefore, we made the following hypothesis: the $L7P^{4+}$ ions at 527 $Å^2$ and 627 $Å^2$ are trans-proline conformations because they are also found in the WT^{4+} spectrum, but the unique $L7P^{4+}$ peak at 610 $Å^2$ is a cis-proline conformation. To test this hypothesis, we performed MD simulations of the 4+ ions.

As a final consideration before MD, we wanted to see if we could detect any conformations in our gas-phase ions that may have originated from their conformations in the

electrospray solvent.[8] The absence or presence of solution-state memory would determine whether we could carry out our simulations entirely in the gas-phase or if simulations in solution would also be necessary. We accomplished this by using collisional activation, similar to methods used by others.[37] The results can be seen in **Figure 3**. Two ATDs are shown for each peptide, one acquired with a 38 V Trap bias and one acquired with a 60 V Trap bias. The Trap bias is the ion optics voltage that injects ions from a low-pressure argon region to the high-pressure helium region near the entrance of the IM cell. Ions injected with a higher bias will be heated to higher temperatures before undergoing collisional cooling in the helium cell.[38] Activation of WT^{4+} and $L7P^{4+}$ ions both result in a decreased population of the compact conformations and an increased population of extended conformations. This indicates that the 527 $Å^2$ conformations may be kinetically trapped intermediates between solution-state and gas phase conformations. We are not making the claim that the compact ions are "solution-like", only that they may represent an intermediate distribution in the unfolding pathway from solution-to-gas-phase. The more extended ions are likely the preferred gas-phase conformations (at our experimental temperature and pressure), and thus we opted to perform all our MD in the gas-phase.

In building our initial MD structures, we first had to determine the protonation sites. The obvious choices in the WT and L7P sequences (**Figure 1A**) were the N-terminus, Lys5, and Arg6. Additionally, the carboxylic acids at Glu27 and the C-terminus were protonated to make them neutral. However, this only produces a 3+ charge, and so the additional protonation of a neutral residue was required. Using a simplified adaptation of Zhang's calculations for gas phase basicities of peptides,[39] we determined that Asn4 was a probable location for sidechain protonation (**N4H**), and Leu25 was probable for backbone amide protonation (**L25H**).

Our computational strategy utilized replica-exchange molecular dynamics (**REMD**) to achieve broad sampling of the conformational space.[40-42] Simulations were performed separately on six initial structures: WT^{4+} (N4H), WT^{4+} (L25H), $L7P^{4+}$ (N4H) with trans-Pro7, $L7P^{4+}$ (N4H) with cis-Pro7, $L7P^{4+}$ (L25H) with trans-Pro7, and $L7P^{4+}$ (L25H) with cis-Pro7. Six REMD runs were initiated, each starting with one of the six initial structures. REMD ran for 100 ns with 34 replicas at temperature windows from 80 K to 1028 K. An exchange was attempted every 100 fs. Snapshot structures from the 300 K windows were output every 22.5 ps, leading to 4444 outputs per starting structure. Each output underwent energy-minimization followed by theoretical CCS calculation using the MOBCAL trajectory method.[43] Structures with theoretical CCS matching within 3% of experimental CCS were kept for conformation cluster analysis by MaxCluster (http://www.sbg.bio.ic.ac.uk/~maxcluster/), a process hereafter referred to as "CCS-filtering." Further computational details can be found in **Supplementary Information 2**.

A summary of the REMD simulations is shown in **Table 1**. No potential was put in place to confine the Arg6-Pro7 bond in cis or trans configuration, and we observed a lot of cis/trans isomerization that initiated in the high temperature windows and trickled down to 300 K. Therefore, we combined all the L7P outputs of the same charge configuration, leading to the four ensembles listed in **Table 1**. With the exception of WT^{4+} (L25H), nearly 50% of the outputs remained after CCS-filtering. Ratios of cis-Pro7 and trans-Pro7 outputs were nearly the same with or without CCS-filtering, with trans-Pro7 structures representing 85% to 95% of the populations. Here, we see the first indications that a cis-proline may not be very favorable for gas-phase $L7P^{4+}$ ions.

Figure S2 contains plots of calculated potential energy of energy-minimized structures versus theoretical CCS for all 300 K REMD outputs. The cis and trans L7P structures are shown

in separate plots. From the distributions, we saw that both WT^{4+} and $L7P^{4+}$ N4H ions cluster much closer to the 527 $Å^2$ experimental CCS. In fact, the N4H ensembles do not contain any theoretical CCS within 3% of the experimental CCS of the more extended ions. Conversely, the distributions of L25H ions are densely distributed towards larger CCS with the exception of some cis-Pro7 structures that form small clusters near both sets of experimental values. We interpreted these data as evidence for differential charge location producing two sets of 4+ ion conformations present in both WT^{4+} and $L7P^{4+}$ IM-MS spectra. Such phenomena has been observed previously for small proteins[44] and large peptides.[45] When a proton is not sequestered by a highly-basic residue, it can be "mobile" and occupy a distribution of protonation sites. Collisional activation can shift the population from one site to another, and the resulting change in charge distribution can cause global conformation changes observable in IM-MS. We hypothesize that during electrospray ionization, or along the gas-phase unfolding pathway, the Asn4 sidechain is the preferred protonation site due to accessibility. When collisionally activated, the proton migrates to the more basic Leu25 backbone amide and reduces coulombic repulsion in the charge-dense N-terminal region.

Initial analysis of the REMD simulations leaves the question of cis/trans isomers in $L7P^{4+}$ unanswered. In fact, with the extended $L7P^{4+}$ conformers only having a 2.7% difference in CCS, they sit right on the edge of being theoretically indistinguishable. Our rationale was that MaxCluster analysis of the CCS-filtered ensembles would reveal whether or not cis and trans structures would form tight, discrete clusters around a particular experimental CCS.

Representative backbone structures of the most populated WT^{4+}, trans $L7P^{4+}$, and cis $L7P^{4+}$ clusters with L25H protonation are shown in **Figure 4**. Backbone ribbons are color-coded to denote the N-terminus (blue) and C-terminus (red). The structures are largely characterized

by an N-terminal hairpin with β-strands from residues 1-5 and 12-15, followed by an elongated middle region and a sharp turn near the C-terminus. Intramolecular solvation of the termini are remarkably similar between Clusters 1, 3, and 5. The charged N-terminal amine is primarily stabilized by neutral carboxylic acids from E27 and the C-term, and some combination of backbones from residues 15-17 provide additional N-term solvation. In Cluster 1, the C-term acid appears to only form polar contacts with the N-term, whereas the C-termini of Cluster 3 and Cluster 5 are close enough to be solvated by the L16 backbone as well. Cluster 6, a cis-proline cluster, is the only L25H cluster that comes within 3% of 527 $Å^2$. While it bears some resemblance to the other double hairpin structures, its broad N-term turn and tangled mid-region cause it to adopt a more globular conformation with a lower CCS.

The WT^{4+} peak at 626 $Å^2$ in **Figure 2** is narrow enough to be explained by a single dominant species, thus we assign it the only dominant Cluster from the CCS-filtered WT^{4+} L25H ensemble, Cluster 1. For the L7P4+ counterpart at 627 Å2, we can assign Cluster 3 (Figure 4), the most highly populated L7P cluster for this system. The assignment of 610 $Å^2$ $L7P^{4+}$ ion is left to two remaining options: the trans-proline Cluster 4 and the cis-proline Cluster 5. The slightly smaller theoretical CCS of Cluster 4 and Cluster 5 is owed to a shallow bend in the peptides' mid-regions, thus making them less extended and more compact. The N-term hairpin peaks at Gly8 in Cluster 3, but the cis-proline of Cluster 5 seems to force the turn one residue earlier at Pro7. In order for the favorable N-term/C-term interactions to still occur, the entire structure must bend in the middle to bring the termini close together. A similar phenomenon could be caused in Cluster 4, as the cap of the N-term hairpin also occurs at Pro7.

Both Clusters 4 and 5 have low relative populations, and both have the same relative difference in theoretical CCS compared to Cluster 3. Combined with the apparent general

instability of cis-Pro7 in $L7P^{4+}$ ions, we are forced to admit that our theoretical evidence suggests the conformation at 610 $Å^2$ may not contain a cis-proline. The hypothesis that the multiple peaks of $L7P^{4+}$ are due to cis/trans proline isomerization is not conclusively supported.

Our $L7P^{4+}$ assignments are summed up in **Figure 5**. Clusters 9 and 11 come from the N4H clusters in **Figure S3**. Their compact shapes likely arise from all charge being densely located near the N-terminus, allowing residues near the C-terminus to provide backbone solvation in globular conformations. Due to similar theoretical CCS and lower relative populations of the dominant clusters, we hypothesize that any of these clusters—or combinations of clusters—could be present in the peak. Additionally, we do not discount the possibility that small amounts of Cluster 6-like structures could be present in that same region. It is interesting to consider the implications of cis and trans structures existing in the narrow peak at 3.0 ms in **Figure 5**. Perhaps the globular nature of the N4H conformations effectively masks what would show up as CCS differences in more elongated conformations.

The extended $L7P^{4+}$ conformation with the largest experimental CCS was assigned Cluster 3, and the assignment of the smaller extended peak remains ambiguous. From the universally low populations of cis structures for $L7P^{4+}$, our inclination is that Cluster 4 is more likely. One could certainly make the argument for a combination of Clusters 4 and 5. In fact, our experimental results from **Figure 3B** show relative Cluster 4/Cluster 3 population ratios of 1:1 and 2:1 under Trap bias settings of 38 V and 60 V, respectively. However, the populations given by REMD in **Figure 4** predict a 1:12 Cluster 4/Cluster 3 ratio. Assuming both Cluster 4 and Cluster 5 exist would then predict a 1:7 ratio, although the agreement between theory and experiment would still not be perfect. Regardless, the fact that evidence suggests cis/trans isomerization may not be the cause for multiple conformations in $L7P^{4+}$ remains unchanged.

Although we are confident in our conclusions, reached after careful examination of the experimental and theoretical evidence, alternatives could be offered. One possibility for the multiple conformations in $L7P^{4+}$ could be additional protonation sites. Just as N4H and L25H configurations lead to different conformations, another backbone or sidechain protonation site, somehow stabilized by the proline-substitution, might do the same. While our data and considerations from Zhang[39] support N4H and L25H as very reasonable assignments, different charge sites would still support the conclusion that our cis/trans isomerization-like experimental data could be explained by alternative phenomena.

If the elongated conformations in the $L7P^{4+}$ ATDs only contain trans peptide bonds between residues 6 and 7, a new question arises: why are WT^{4+} ions unable to display two extended conformations? It is possible that the intrinsic rigidity of proline—whether cis or trans—stabilizes the N-term hairpin's apex at the seventh residue. Thus, WT4+ might always produce a turn with the apex at Gly8 and never be forced to bend its elongated backbone for the N-term/C-term interactions. This, of course, is just speculation. The effect of proline-substitution on other peptides with N-terminal and C-terminal turns would provide an interesting system for future experiments.

All evidence considered, the answer to the question posed by our title, "is it always cis/trans isomerization?" is no. To be fair, however, previous investigations never claimed it was. Our aim was to explicitly demonstrate that systems with uncanny experimental resemblance to the cis/trans isomerization "signature" can reveal a different origin when investigated further. One cannot solely rely on experimental IM-MS data for structural analysis. This study should not be seen as refutation of any previously published IM-MS cis/trans assignments, as many of those investigations do provide theoretical validation. Some

experiments even utilized additional MS methods for validation, such as ultraviolet photodissociation[15-16] and ion spectroscopy,[12] which can take an investigation much further than MD alone. As more researchers utilize IM-MS for cis/trans analysis, we encourage that trend to continue.

Acknowledgements

This work is supported in part by the National Science Foundation grant (CHE-1413596 to LL, CHE-1300209 to QC, CHE-0840494 to the UW Phoenix cluster) and the National Institutes of Health grants (1R01DK071801 and 1R56DK071801 to LL). The computational research was performed, in part, using the computing resources and assistance of the UW-Madison Center For High Throughput Computing (CHTC) in the Department of Computer Sciences. The CHTC is supported by UW-Madison, the Advanced Computing Initiative, the Wisconsin Alumni Research Foundation, the Wisconsin Institutes for Discovery, and the National Science Foundation, and is an active member of the Open Science Grid, which is supported by the National Science Foundation and the U.S. Department of Energy's Office of Science. C.L. acknowledges an NIH-supported Chemistry Biology Interface Training Program Predoctoral Fellowship (grant number T32-GM008505) and an NSF Graduate Research Fellowship (DGE-1256259). LL acknowledges an H. I. Romnes Faculty Research Fellowship. The authors would also like to thank Dr. Matthew S. Glover (UW – Madison) for his helpful insights and discussions.

References

(1) H. E. Revercomb, and E. A. Mason, *Analytical Chemistry*, 1975, **47**, 970-983.
(2) G. von Helden, T. Wyttenbach, and M. T. Bowers, *Science*, 1995, **267**, 1483-1485.
(3) D. E. Clemmer, R. R. Hudgins, and M. F. Jarrold, *Journal of the American Chemical Society*, 1995, **117**, 10141-10142.
(4) J. A. McLean, B. T. Ruotolo, K. J. Gillig, and D. H. Russell, *International Journal of Mass Spectrometry*, 2005, **240**, 301-315.
(5) J. L. P. Benesch, and B. T. Ruotolo, *Current Opinion in Structural Biology*, 2011, **21**, 641-649.
(6) E. Jurneczko, and P. E. Barran, *Analyst*, 2011, **136**, 20-28.
(7) F. Lanucara, S. W. Holman, C. J. Gray, and C. E. Eyers, *Nat Chem*, 2014, **6**, 281-294.
(8) N. A. Pierson, L. Chen, S. J. Valentine, D. H. Russell, and D. E. Clemmer, *Journal of the American Chemical Society*, 2011, **133**, 13810-13813.
(9) A. E. Counterman, and D. E. Clemmer, *Journal of Physical Chemistry B*, 2004, **108**, 4885-4898.
(10) T. Y. Kim, S. J. Valentine, D. E. Clemmer, and J. P. Reilly, *Journal of the American Society for Mass Spectrometry*, 2010, **21**, 1455-1465.
(11) L. Shi, A. E. Holliday, M. S. Glover, M. A. Ewing, D. H. Russell, and D. E. Clemmer, *J Am Soc Mass Spectrom*, 2015.
(12) A. Masson, M. Z. Kamrath, M. A. S. Perez, M. S. Glover, U. Rothlisberger, D. E. Clemmer *et al.*, *Journal of the American Society for Mass Spectrometry*, 2015, **26**, 1444-1454.
(13) C. B. Lietz, Q. Yu, and L. J. Li, *Journal of the American Society for Mass Spectrometry*, 2014, **25**, 2009-2019.
(14) A. E. Counterman, and D. E. Clemmer, *Journal of the American Chemical Society*, 2001, **123**, 1490-1498.
(15) S. Warnke, C. Baldauf, M. T. Bowers, K. Pagel, and G. von Helden, *Journal of the American Chemical Society*, 2014, **136**, 10308-10314.
(16) S. Warnke, G. von Helden, and K. Pagel, *Proteomics*, 2015, **15**, 2804-2812.
(17) T. G. Flick, I. D. G. Campuzano, and M. D. Bartberger, *Analytical Chemistry*, 2015, **87**, 3300-3307.
(18) A. E. Counterman, and D. E. Clemmer, *Analytical Chemistry*, 2002, **74**, 1946-1951.
(19) N. A. Pierson, L. Chen, D. H. Russell, and D. E. Clemmer, *J Am Chem Soc*, 2013, **135**, 3186-3192.
(20) W. J. Wedemeyer, E. Welker, and H. A. Scheraga, *Biochemistry*, 2002, **41**, 14637-14644.
(21) N. A. Pierson, and D. E. Clemmer, *Int J Mass Spectrom*, 2015, **377**, 646-654.
(22) M. S. Glover, L. Shi, D. R. Fuller, R. J. Arnold, P. Radivojac, and D. E. Clemmer, *J Am Soc Mass Spectrom*, 2015, **26**, 444-452.
(23) M. S. Glover, E. P. Bellinger, P. Radivojac, and D. E. Clemmer, *Anal Chem*, 2015, **87**, 8466-8472.
(24) L. Tao, D. Dahl, L. Pérez, and D. Russell, *Journal of the American Society for Mass Spectrometry*, 2009, **20**, 1593-1602.
(25) F. A. Fernandez-Lima, H. Wei, Y. Q. Gao, and D. H. Russell, *The Journal of Physical Chemistry A*, 2009, **113**, 8221-8234.
(26) T. Wyttenbach, N. A. Pierson, D. E. Clemmer, and M. T. Bowers, *Annual Review of Physical Chemistry*, 2014, **65**, 175-196.
(27) T. Pedrazzini, F. Pralong, and E. Grouzmann, *Cell Mol Life Sci*, 2003, **60**, 350-377.
(28) M. K. Karvonen, U. Pesonen, M. Koulu, L. Niskanen, M. Laakso, A. Rissanen *et al.*, *Nat Med*, 1998, **4**, 1434-1437.
(29) G. C. Mitchell, Q. Wang, P. Ramamoorthy, and M. D. Whim, *J Neurosci*, 2008, **28**, 14428-14434.
(30) O. Ukkola, and Y. A. Kesaniemi, *Eur J Clin Nutr*, 2007, **61**, 1102-1105.
(31) B. Ding, B. Kull, Z. Liu, S. Mottagui-Tabar, H. Thonberg, H. F. Gu *et al.*, *Regulatory Peptides*, 2005, **127**, 45-53.

(32) A. A. Shvartsburg, and R. D. Smith, *Analytical Chemistry*, 2008, **80**, 9689-9699.
(33) B. T. Ruotolo, J. L. P. Benesch, A. M. Sandercock, S.-J. Hyung, and C. V. Robinson, *Nat. Protocols*, 2008, **3**, 1139-1152.
(34) D. Smith, T. Knapman, I. Campuzano, R. Malham, J. Berryman, S. Radford *et al.*, *European Journal of Mass Spectrometry*, 2009, **15**, 113-130.
(35) M. F. Bush, I. D. G. Campuzano, and C. V. Robinson, *Analytical Chemistry*, 2012, **84**, 7124-7130.
(36) Y. Zhong, S. J. Hyung, and B. T. Ruotolo, *Analyst*, 2011, **136**, 3534-3541.
(37) N. A. Pierson, S. J. Valentine, and D. E. Clemmer, *The Journal of Physical Chemistry B*, 2010, **114**, 7777-7783.
(38) S. Merenbloom, T. Flick, and E. Williams, *Journal of The American Society for Mass Spectrometry*, 2012, **23**, 553-562.
(39) Z. Zhang, *Analytical Chemistry*, 2004, **76**, 3908-3922.
(40) A. Baumketner, S. L. Bernstein, T. Wyttenbach, G. Bitan, D. B. Teplow, M. T. Bowers *et al.*, *Protein Science*, 2006, **15**, 420-428.
(41) F. Albrieux, F. Calvo, F. Chirot, A. Vorobyev, Y. O. Tsybin, V. Lepère *et al.*, *The Journal of Physical Chemistry A*, 2010, **114**, 6888-6896.
(42) F. Chirot, F. Calvo, F. Albrieux, J. Lemoine, Y. Tsybin, and P. Dugourd, *Journal of The American Society for Mass Spectrometry*, 2012, **23**, 386-396.
(43) M. F. Mesleh, J. M. Hunter, A. A. Shvartsburg, G. C. Schatz, and M. F. Jarrold, *The Journal of Physical Chemistry*, 1996, **100**, 16082-16086.
(44) B. C. Bohrer, N. Atlasevich, and D. E. Clemmer, *Journal of Physical Chemistry B*, 2011, **115**, 4509-4515.
(45) A. E. Counterman, and D. E. Clemmer, *Journal of Physical Chemistry B*, 2003, **107**, 2111-2117.

Table 1. Summary of outputs from REMD simulations

Ensemble	Total Population	Total TRANS/CIS	CCS-filtered Population	CCS-filtered TRANS/CIS
WT^{4+} (N4H)	4444	-	2513 (56.5%)	-
$L7P^{4+}$ (N4H)	8888	7931/957 (89.2%,10.8%)	4565 (51.3%)	3870/695 (84.8%/15.2%)
WT^{4+} (L25H)	4444	-	758 (17%)	-
$L7P^{4+}$ (L25H)	8888	8040/848 (90.4%/9.6%)	4240 (47.7%)	3760/480 (88.7%/11.3%)

Figure Legends

Figure 1. Mass spectrometry of WT and L7P peptides. A) The sequences of WT and L7P, which only differ in the identity of the seventh residue (highlighted in red). **B)** The individual direct-infusion nano electrospray ionization mass spectra of WT and L7P. Insets of spectral regions containing 4+ ions (highlighted in yellow) and 2+ ions (highlighted in green) are shown below in **C) – D)** and **E) – F)**, respectively. For these spectra, WT and L7P were analyzed separately. For all other experiments and spectra, they were analyzed as a mixture.

Figure 2. ATDs and calibrated CCS for 4+ peptide ions. ATDs were acquired at IM cell wave height and wave velocity settings of 40 V and 600 m s^{-1}, respectively. Reported CCS are mean values from calibrations and measurements taken at several different wave heights and wave velocities.

Figure 3. Collisional activation of 4+ peptide ions. ATDs of **A)** WT^{4+} and **B)** $L7P^{4+}$ ions resulting from measurements taken with Trap Bias settings of 38 V and 60 V. ATDs were acquired at IM cell wave height and wave velocity settings of 40 V and 600 m s^{-1}, respectively. Reported CCS are mean values from calibrations and measurements taken at several different wave heights and wave velocities.

Figure 4. Candidate structures for L25H 4+ ions. Representative centroid structures from the highest population conformation clusters of **A)** WT^{4+} and **B)** $L7P^{4+}$ L25H ions. Atoms from the entire backbone and seventh residue's sidechain are displayed. Structures are color-coded to denote N-terminal (blue) and C-terminal (red) regions. Relative cluster population and mean

theoretical CCS of the cluster are listed below the centroid structure. The total populations of the WT^{4+} and $L7P^{4+}$ L25H CCS-filtered ensembles were 758 and 4240, respectively.

Figure 5. Putative structural assignments for $L7P^{4+}$ ions. Representative cluster centroids are shown by the $L7P^{4+}$ ATD to which they were putatively assigned. Identity of the proline-type for the peak near 3.8 ms remains ambiguous. ATDs were acquired at IM cell wave height and wave velocity settings of 40 V and 600 m s^{-1}, respectively.

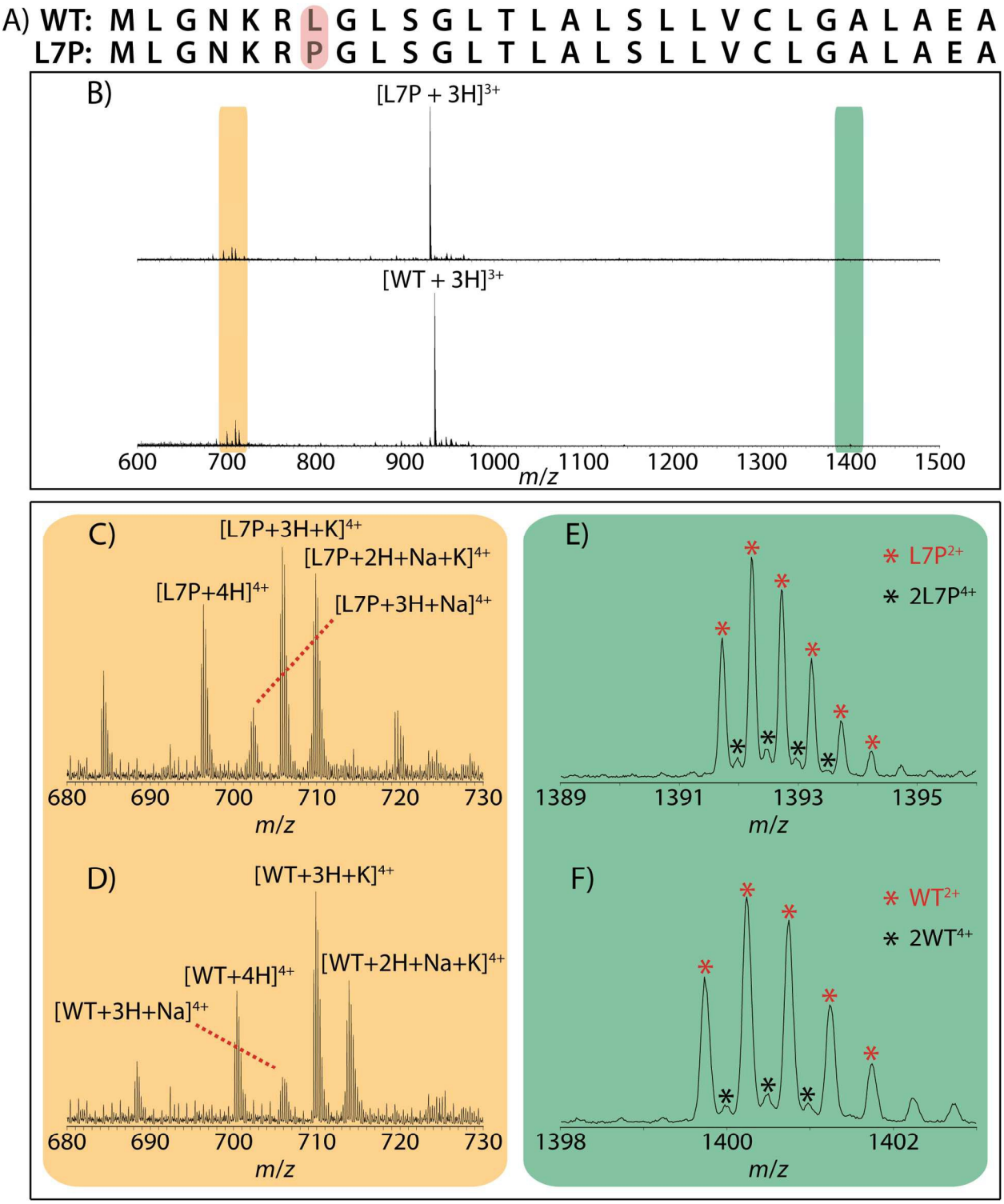

Lietz et al., Figure 1

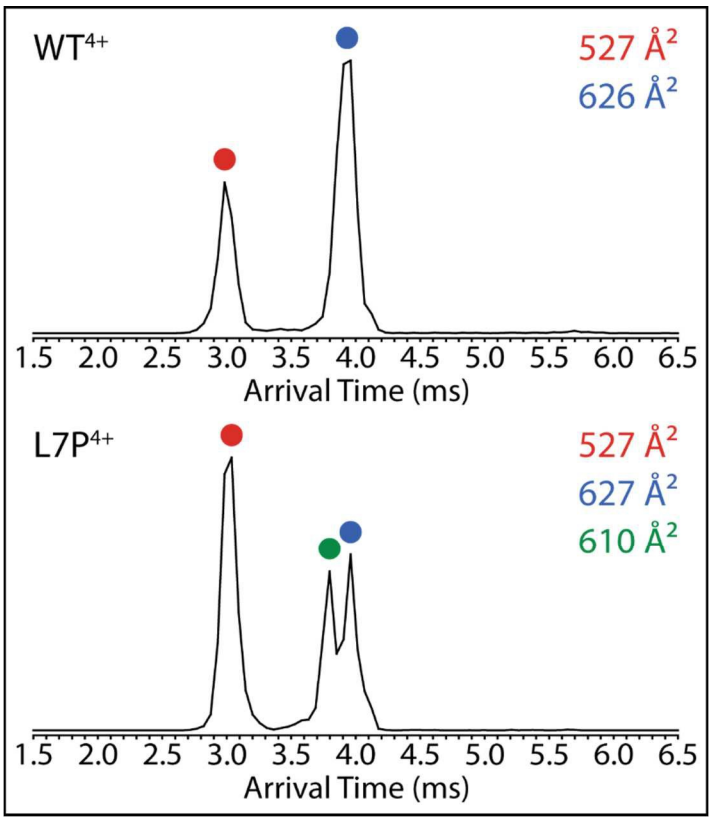

Lietz et al., Figure 2

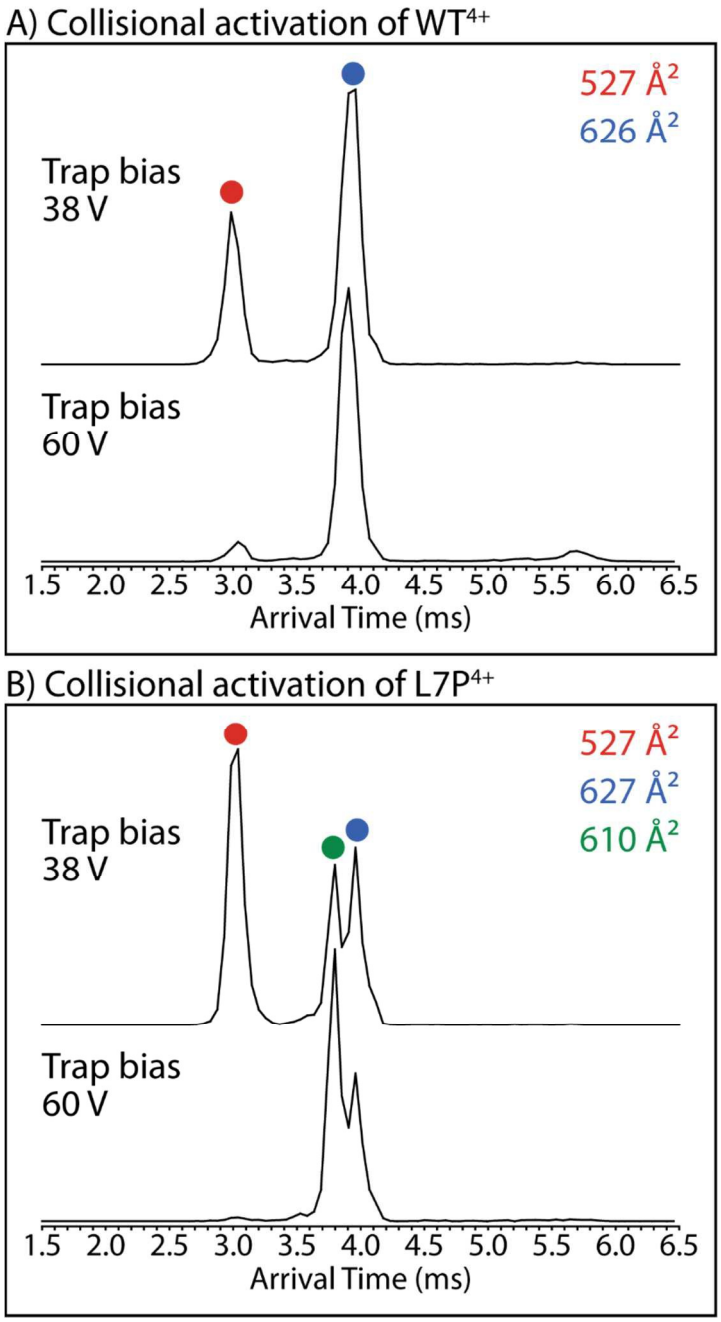

Lietz et al., Figure 3

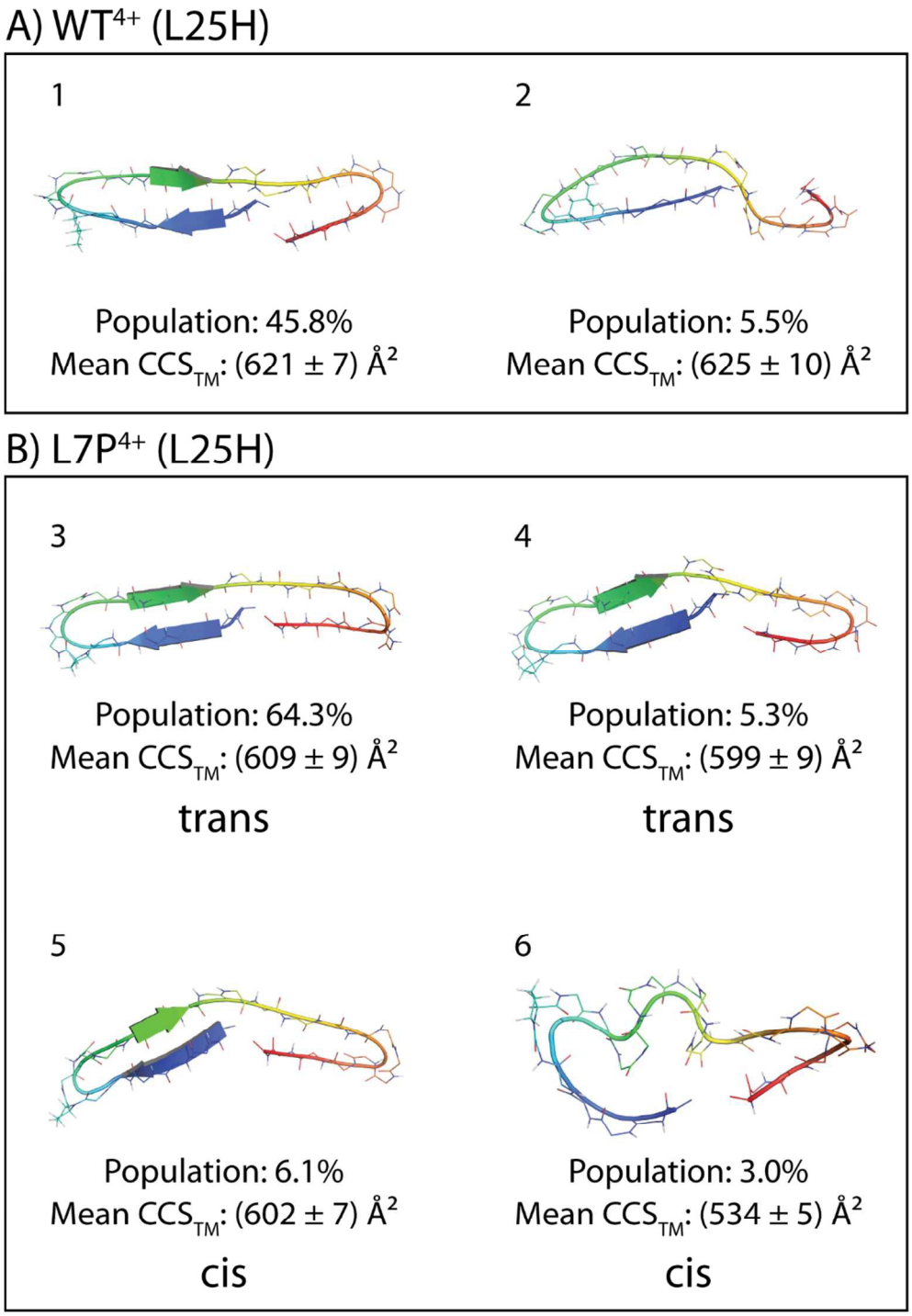

Lietz et al., Figure 4

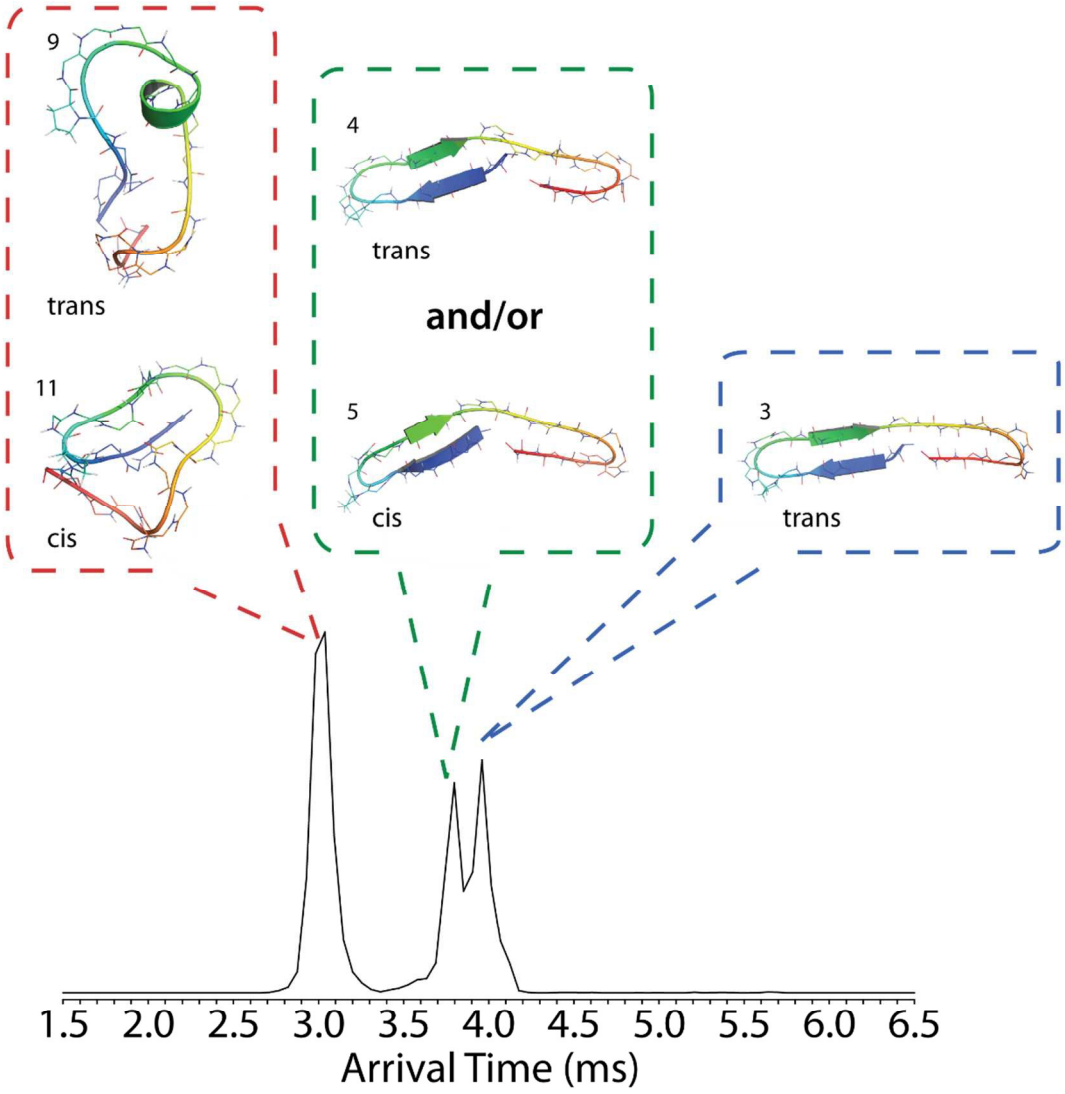

Lietz et al., Figure 5